AN ALGORITHM FOR VERICATION AND CHANGE DETECTION BETWEEN 3D GEOSPATIAL DATABASES AND AERIAL IMAGES

Thomas Knudsen

Danish National Space Center, Juliane Maries Vej 30, 2100 Copenhagen Ø, Denmark, tk@spacecenter.dk

KEY WORDS: building detection, change detection, TOP10DK, unsupervised segmentation, covariance matrices

ABSTRACT:

An algorithm for building detection in aerial images is presented. The algorithm is based on a combination of unsupervised segmentation and selection of a training set based on existing building registrations. The classification/detection step is based on individual comparison of the segments, represented by their covariance matrices, which are compared using a suitable metric.

1 INTRODUCTION

Buildings are some of the most important mapping objects so it is not surprising that in the last decade a number of algorithms for automated registration of buildings in aerial images, have appeared (e.g. Baltsavias, 2002; Fischer et al., 1999, 1998; Matikainen et al., 2003; Niederöst, 2003; Süveg, 2003; Süveg and Vosselman, 2004; Walter, 2004). These algorithms do however, in general depend on the availability of good first guesses for the 2D image coordinates of potential buildings.

As noted by Baltsavias (2004), generating the first guesses is far from trivial where no previous registrations are available, i.e. in the case of new objects. Nevertheless, the primary aim of this paper is to present a simple algorithm for change detection in the building theme of a digital map database—a task which can be broken down to two related sub-tasks:

1. to verify the existing registrations; and
2. to generate first guesses for the position of new buildings.

Much of the work presented here is simplified by using fully three dimensional map registrations which, contrary to 2D registrations, can be projected directly onto a new set of aerial images used in the update process.

2 DATA

As indicated above this study is based on a combination of vector data from an existing GIS database, and aerial image data aquired in order to update/revise the GIS data. The GIS data are extracted from the *TOP10DK* database, while the aerial images come from flight campaigns using the Vexcel UltraCam large format digital camera.

2.1 TOP10DK—a GIS database

The TOP10DK database is the primary base product for official maps of Denmark at the scales 1:10 000–1:250 000. It was originally compiled under contracts from the National Survey and Cadastre of Denmark in the years 1997–2001 and defines 52 object types (highway, road, house, etc) organized in 8 object classes (traffic, building, water, etc). The original data capture was based on stereo registration from aerial photos resulting in a fully 3D data set with an accuracy significantly better than 1 m in all directions (Kort & Matrikelstyrelsen, 2001).

The maintenance cycle for TOP10DK is 5 years, but a shorter cycle for the most important objects (roads, buildings) is under consideration. This is a major motivational factor for the present work, since anything that could automate parts of the production cycle will be of importance in reaching this goal.

2.2 The Vexcel UltraCam camera

The original release of the Vexcel Ultracam digital aerial frame camera has a focal length of approximately 100 mm. Its panchromatic channel has a pixel size of $9\mu m$ square, an across track size of 11500 pixels and an along track size of 7500 pixels. For a flying height of 4000 m this gives a nominal coverage of 4140 m by 2700 m and a ground sample distance of 0.36 m, which is comparable to a traditional analog image scanned at 15–20 μm.

The four colour channels (near-infrared, N, red, R, green, N, and blue, B) are registered at half resolution, but later in the process pan-sharpened to pseudo-full-resolution (Leberl et al., 2003).

In the present work, the availability of a near-infrared channel is very important for discriminating between vegetation covered and man made surfaces. This leads to a major reduction of data dimensionality.

2.3 Flight Campaigns

The data shown in figures 1–2are from a flight near the city of Odense in the central part of Denmark. The scenes used were shot on 2005-04-02, around 13:00 central european daylight savings time—very close to local noon, i.e. with a high solar elevation. The nominal flight height was 4020 m, for a nominal ground sample distance (GSD) of 35 cm

The data shown in figure 3 are from a flight covering the southern suburbs of Copenhagen, in the eastern part of Denmark. The scenes used were shot on 2006-05-06, around 09:00 central european daylight savings time—i.e with a low solar elevation. The nominal flight height was 1185 m, for a nominal GSD of 10 cm

3 ALGORITHM

Presented at a reasonable level of detail, the change detection algorithm consists of nine steps going from data capture to final change map

1. shoot an aerial photo.

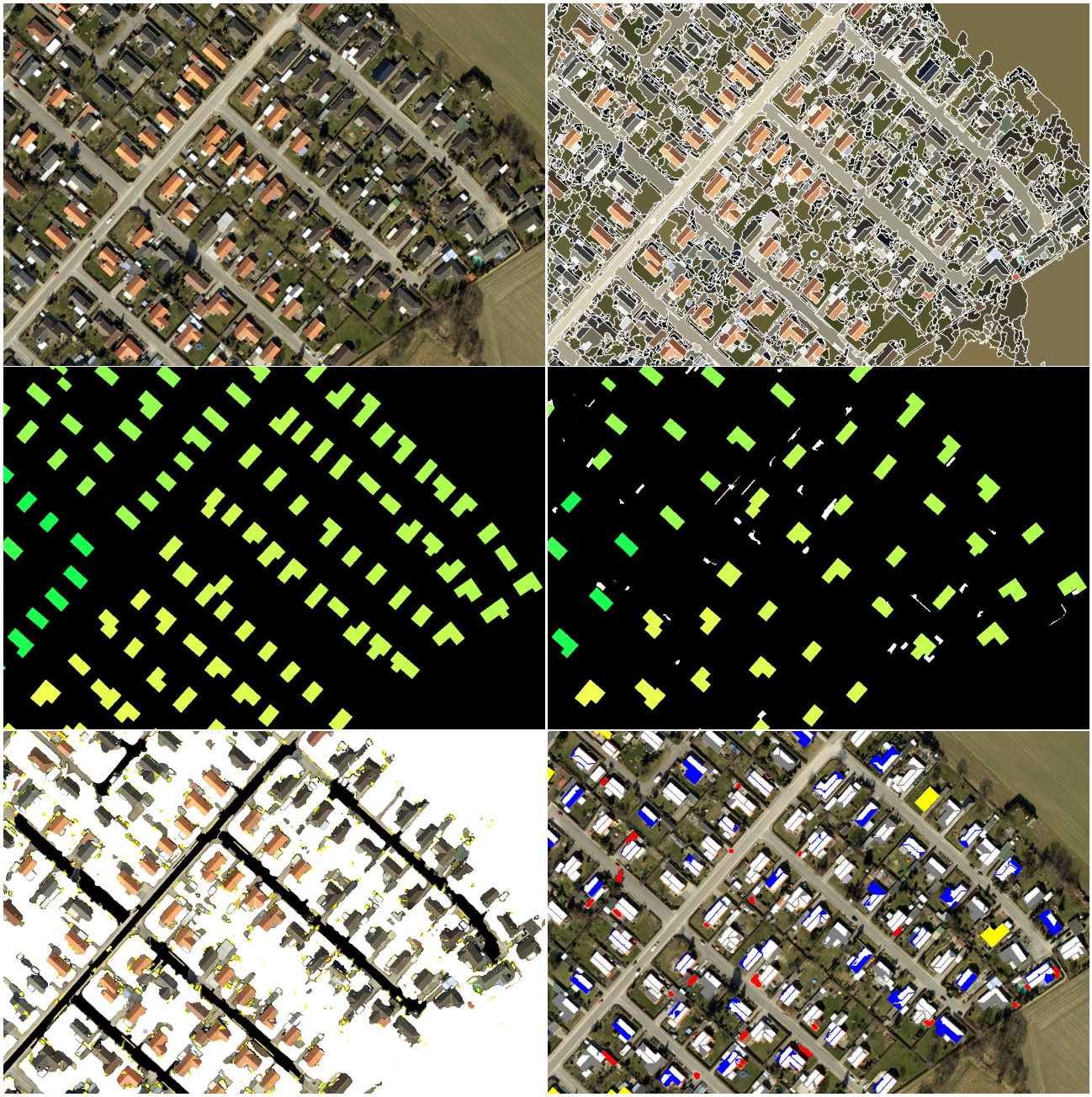

Figure 1: Some steps from a test case. Upper row: the original image and the segmented image. Center row: original building registrations and the distorted dataset used for algorithm verification. Lower row: removal of vegetation covered areas and final result (see text for the meaning of the colour coding). This scene was shot at high solar elevation with a nominal GSD of 35 cm; its size is 1102×737 pixels for a nominal ground coverage of $386\,\mathrm{m} \times 258\,\mathrm{m}$

2. image segmentation.
3. projection of the existing 3D registrations onto the photo
4. compute gradient and vegetation index images
5. remove obvious "non-building" segments from the image using reasoning based on size and vegetation index.
6. for each segment, compute a 7x7 covariance matrix from the cluster of associated NRGB+row+column+gradient values
7. for each segment, find the N segments with the most similar covariance matrices
8. detect buildings by majority vote: if the majority of the N most similar segments are already registered as buildings, then the current segment is "elected as a member of the building class"
9. find changes by comparing with the set of existing registrations

The image segmentation in step 2 is carried out using the EDISON algorithm by Christoudias et al. (2002), which in prior studies have shown to result in cartographically meaningful segmentations.

In step 6 we combine the colour vector with row and column coordinates and the intensity gradient in order to get shape and texture information represented in some of the off diagonal cells of the covariance matrix.

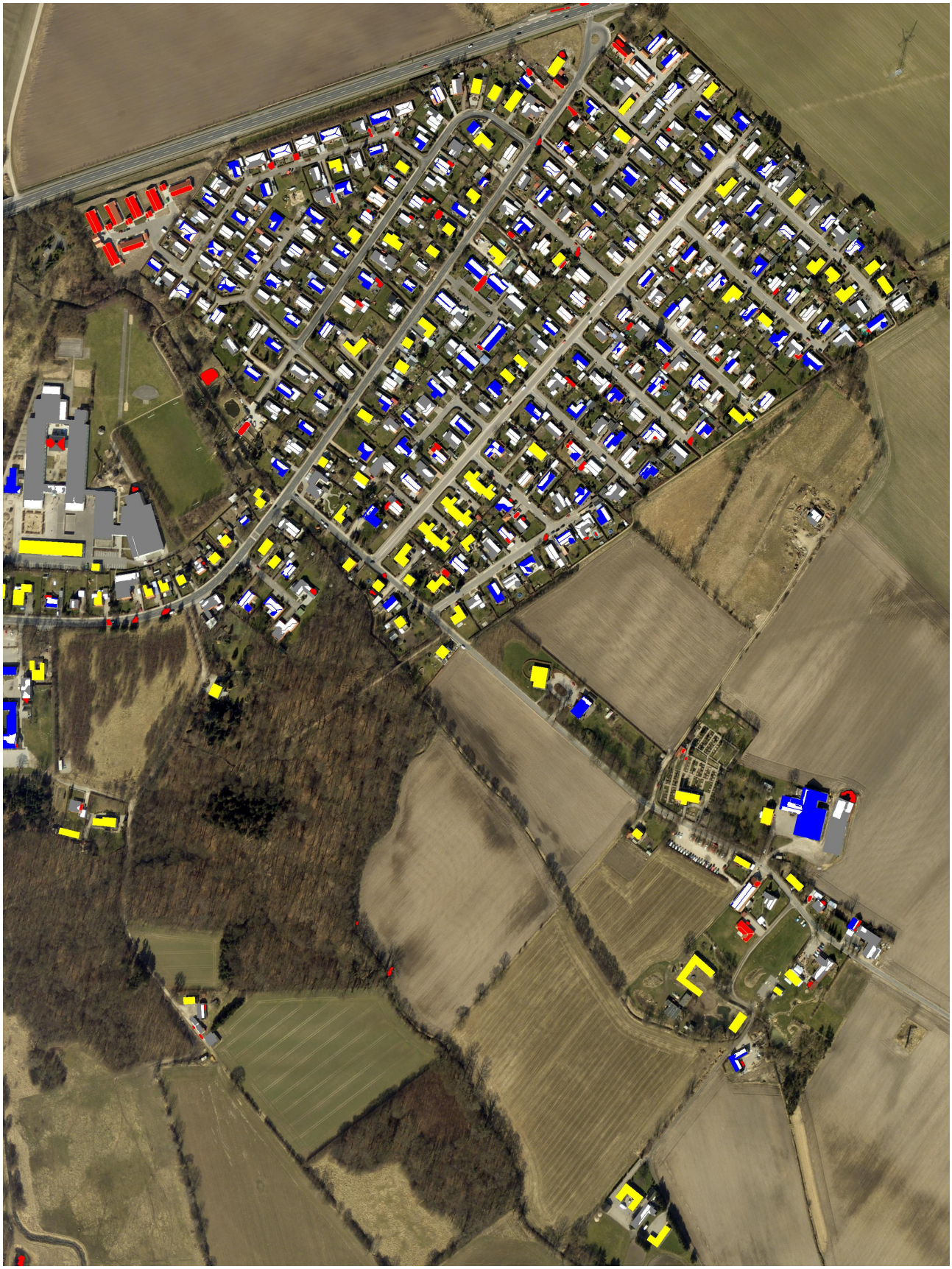

Figure 2: A 12-fold extended test-area, including the area shown in figure 1. This scene was shot at high solar elevation with a nominal GSD of 35 cm; its size is 2700×3600 pixels for a nominal ground coverage of $945\,\mathrm{m} \times 1260\,\mathrm{m}$

In step 7 we need a distance metric to determine which covariance matrices are most similar. Currently, we use the metric derived by Förstner and Moonen (1999) which computes a distance, d,

between two covariance matrices, C_1 and C_2 as:

$$d(\mathbf{C}_1,\mathbf{C}_2) = \sqrt{\sum_{i=1}^{n} ln^2\lambda_i(\mathbf{C}_1,\mathbf{C}_2)}$$

Where λ_i are the eigenvalues of the generalized eigenvalue problem involving the two covariance matrices:

$$\lambda_i\mathbf{C}_1\mathbf{x}_i - \mathbf{C}_2\mathbf{x}_i = 0$$

A similar procedure was used by Tuzel et al. (2006) for pixel-wise classification based on covariance matrices of rectangular regions around each pixel. Here, we compute the covariance matrices within the pixel clusters defined by the image segmentation algorithm. This has two advantages over the pixel-wise method: first and foremost, we get a significant reduction of the number of covariance matrices to consider (one for each cluster vs. one for each pixel), second, we avoid computing covariance matrices for areas covering more than one domain (i.e. surface type), which is inevitable when operating within rectangular regions.

4 RESULTS

4.1 Initial results

Figure 1 shows some of the steps for a case study involving a 10 hectare suburban test area in central Denmark. The original image consists of 737 rows by 1102 columns, i.e. 812 174 pixels. After segmentation, this is reduced to 4 432 clusters. After removal of vegetation covered areas, we are down to 799 clusters, i.e. more than a factor of 1 000 less than the original 812 174 pixels.

Initially, 102 buildings were registered in the area. To check the algorithm, we remove 50 of them (the validation set). To further check the stability of the algorithm, we add a set of 45 non-building clusters to the training set ("misregistrations").

The results are shown in the lower right panel of the figure with the following colour coding:

grey	non-detected parts of the training set.
blue	non-detected parts of the validation set.
white	detected parts of both sets.
yellow	buildings which are not even partially detected.
red	false alarms: non-buildings detected as buildings.

Of the initially registered 102 buildings, we removed 50. We have (at least partially) redetected 96 of the 102 total, and 49 of the 50 removed.

Of the remaining 6 undetected buildings, 4 are really tiny corners of buildings on the edge of the image. Hence it could be argued that the total score is really 96 out of 98 rather than 96 out of 102.

One of the two non edge cases of fully undetected buildings, is fitted with a highly unusual blue roof and pinpoints one of the major weaknesses of the algorithm: new roofing materials, which are not properly described in the training set will not be detected.

The group of false alarms, 42 all in all, marked up in red in the figure, consists of a combination of

1. plain false alarms
2. sheds/carports which are not registered in the TOP10DK database, but which look like ordinary buildings when viewed from above
3. re-detected misregistrations
4. protruding building parts which have been generalized away in the original registration

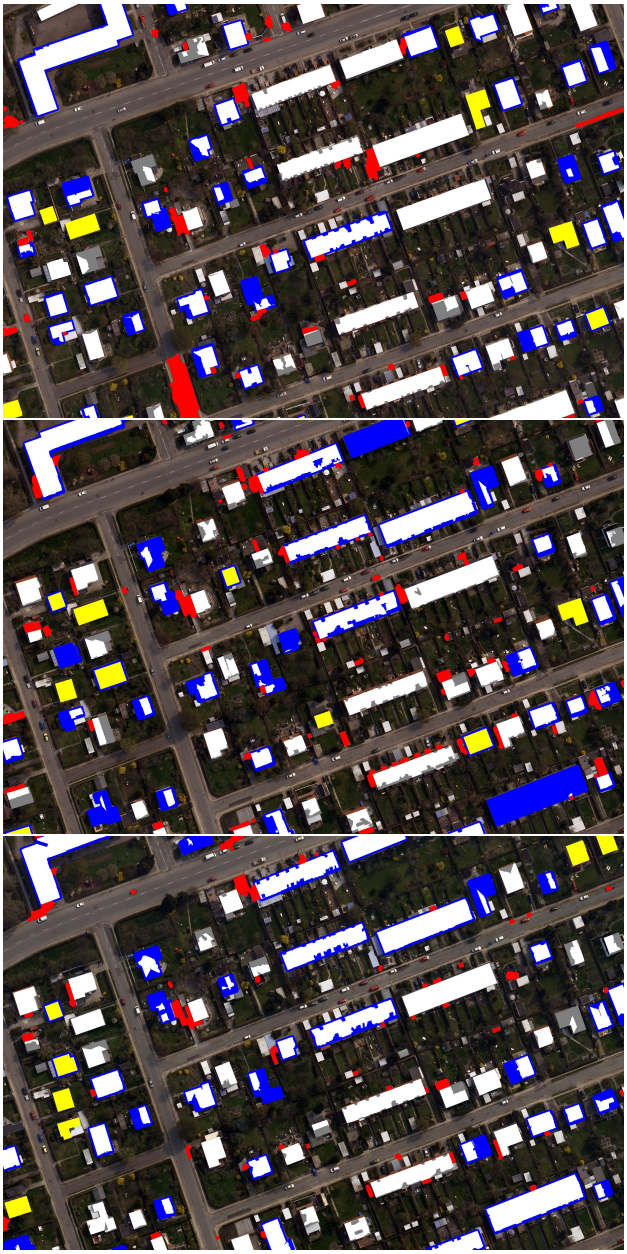

Figure 3: Results from three views of the same area (cut from three consecutive scenes along the flight track). These scenes were shot at low solar elevation with a nominal GSD of 10 cm; their size is 3000×2000 pixels each, for a nominal ground coverage of $300\,\mathrm{m} \times 200\,\mathrm{m}$

A number of these can be eliminated by morphological filtering and shape and size considerations.

While the test case presented above admittedly covers a small area in a suburban setting, where the algorithm is expected to perform at its optimum due to the good contrast between buildings and surrounding vegetation, the results really are quite convincing: detecting 98% of the validation data set is not bad.

4.2 Results from a larger area

Figure 1 shows the results from an experiment where the test area from figure 1 was extended heavily.

In this case, the detection of new buildings is still going very well, including detecting a group of 7 houses in the upper left corner, which are marked in red. This indicates that they were not deliberately removed from the database: they were actually not yet registered.

The redetection of existing registrations is less succesful than in the previous case. This is probably due to the fact that large patches of field is still not vegetation covered. Apparently, this leads to a number of segments having similar spectral characteristics as roofing felt covered roofs. This indicates that it is actually a good idea to do an initial screening of the areas included in the procedure: here we have effectively included large rural areas in a dataset used with an algorithm specificly intended for suburban areas.

4.3 Varying flying height and solar elevation

The data in figure 3 comes from three different (but subsequent) scenes covering the same area. In this case, we operate at very low solar elevation (the photos were shot at 09:00 in the morning), and very high spatial resolution (GSD 10 cm).

In this case, it is worth noting that there are differences between the results in the three cases. This indicates that combining evidence from the individual scenes could lead to much more stable results in the case of low solar elevation, where the spectral response of the surface materials is less well defined.

5 CONCLUSION

In the initial test case (which had an optimum setting: truly suburban coverage, good solar elevation) the algorithm presented worked very well, both in terms of validation (98%) and verification.

When degrading the homogeneity of the coverage, performance was also reduced—especially with respect to redetection.

At lower solar elevation similar effects were seen. It is however also evident that the potential high number of overlaps feasible from digital cameras can help remedy this by utilizing a combination of evidence from each scene.

All in all, while still needing additional refinement and characterisation, the method presented seems promising.

ACKNOWLEDGEMENTS

Map and image data for this study were provided by the National Survey and Cadastre—Denmark (Kort & Matrikelstyrelsen/KMS). In particular, the author wishes to thank Brian Pilemann Olsen and Rune Carbuhn Andersen of KMS, both of whom (despite having a plethora of other tasks to handle in their everyday work), have taken special interest in making the material used here available, as well as taking time and interest in commenting on the results reported.

References

Baltsavias, E., 2002. Object extraction and revision by image analysis using existing geospatial data and knowledge: state-of-the-art and steps towards operational systems. International archives of photogrammetry, remote sensing and spatial information sciences XXXIV(2), pp. 13–22.

Baltsavias, E. P., 2004. Object extraction and revision by image analysis using existing geodata and knowledge: current status and steps towards operational systems. ISPRS Journal of Photogrammetry and Remote Sensing 58, pp. 129–151.

Christoudias, C. M., Georgescu, B. and Meer, P., 2002. Synergism in low level vision. In: 16th International Conference on Pattern Recognition. Track 1: Computer Vision and Robotics, Quebec City, Canada, Vol. IV, pp. 150–155.

Fischer, A., Kolbe, T. H. and Lang, F., 1999. On the use of geometric and semantic models for component-based building reconstruction. In: W. Förstner, C.-E. Liedtke and J. Bückner (eds), Semantic Modeling for the Acquisition of Topographic Information from Images and Maps SMATI '99, Institut für Photogrammetrie, Universität Bonn, Institut für Photogrammetrie, Universität Bonn, pp. 101–119.

Fischer, A., Kolbe, T., Lang, F., Cremers, A., Förstner, W., Plümer, L. and Steinhage, V., 1998. Extracting buildings from aerial images using hierarchical aggregation in 2d and 3d. Computer Vision and Image Understanding 72(2), pp. 185–203.

Förstner, W. and Moonen, B., 1999. A metric for covariance matrices. In: F. Krumm and V. S. Schwarze (eds), Quo vadis geodesia...? Festschrift for Erik W. Grafarend on the occasion of his 60th birthday, Schriftenreihe der Institute des Studiengangs Geodäsie und Geoinformatik, Universität Stuttgart, pp. 113–128.

Kort & Matrikelstyrelsen, 2001. TOP10DK geometrisk registrering, specifikation udgave 3.2.0. Copenhagen, Denmark: Kort & Matrikelstyrelsen.

Leberl, F., Gruber, M., Ponticelli, M., Bernögger, S. and Perko, R., 2003. The UltraCam large format aerial digital camera system. In: Proceedings of the ASPRS Annual Convention, Anchorage, USA, 2003.

Matikainen, L., Hyyppä, J. and Hyyppä, J., 2003. Automatic detection of buildings from laser scanner data for map updating. In: ISPRS Commission III. Workshop 3-d reconstruction from airborne laserscanner and InSAR data, p. 8.

Niederöst, M., 2003. Detection and Reconstruction of Buildings for Automated Map Updating. PhD thesis, Institut für Geodäsie und Photogrammetrie, Eidgenössische Technische Hochschule Zürich, ETH Hönggerberg, Zürich.

Süveg, I., 2003. Reconstruction of 3D Building Models from Aerial Images and Maps. Publications on Geodesy, Netherlands Geodetic Commision, Delft, the Netherlands.

Süveg, I. and Vosselman, G., 2004. Reconstruction of 3D building models from aerial images and maps. ISPRS Journal of Photogrammetry and Remote Sensing 58, pp. 202–224.

Tuzel, O., Porikli, F. and Meer, P., 2006. Region covariance: A fast descriptor for detection and classification. In: A. Leonardis, H. Bischof and A. Prinz (eds), ECCV 2006, Part II, LNCS 3952, pp. 589–600.

Walter, V., 2004. Object-based classification of remote sensing data for change detection. ISPRS Journal of Photogrammetry and Remote Sensing 58, pp. 225–238.